Chinese J. Chem. Eng., **11** (3) 302 – 306 (2003)

Kinetics and Mechanism of Decomposition of Nano-sized Calcium Carbonate under Non-isothermal Condition*

LIU Runjing(刘润静)[a], CHEN Jianfeng(陈建峰)[a,], GUO Fen(郭奋)[a], YUN Jimmy(吉米)[b] and SHEN Zhigang(沈志刚)[a]**

[a] Research Center of the Ministry of Education for High Gravity Engineering and Technology, Beijing University of Chemical Technology, Beijing 100029, China

[b] NanoMaterials Technology Pte Ltd., Block 26, Ayer Rajah Crescent # 07—02, Singapore 1339944

Abstract Experiments on thermal decomposition of nano-sized calcium carbonate were carried out in a thermogravimetric analyzer under non-isothermal condition of different heating rates (5 to 20 $K \cdot min^{-1}$). The Coats and Redfern's equation was used to determine the apparent activation energy and the pre-exponential factors. The mechanism of thermal decomposition was evaluated using the master plots, Coats and Redfern's equation and the kinetic compensation law. It was found that the thermal decomposition property of nano-sized calcium carbonate was different from that of bulk calcite. Nano-sized calcium carbonate began to decompose at 640°C, which was 180°C lower than the reported value for calcite. The experimental results of kinetics were compatible with the mechanism of one-dimensional phase boundary movement. The apparent activation energy of nano-sized calcium carbonate was estimated to be 151 $kJ \cdot mol^{-1}$ while the literature value for normal calcite was approximately 200 $kJ \cdot mol^{-1}$. The order of magnitude of pre-exponential factors was estimated to be 10^9 s^{-1}.

Keywords nano-sized calcium carbonate, non-isothermal decomposition, kinetic mechanism

1 INTRODUCTION

Solid state decomposition reactions are one of the important fields in solid chemistry. The coal pyrolytic kinetics[1], the kinetic behavior and process of thermal decomposition of α-zirconium phosphate[2], the thermal decomposition of propellant[3], the crystallization kinetics of aleic anhydride graft polypropylene[4] have been reported. Nano-sized $CaCO_3$ as functional materials has been widely used in nanocomposites such as rubbers, plastics and coating. In processes of polymers, thermal stability of nano-sized $CaCO_3$ is very important. Nano-sized $CaCO_3$ as template has been applied in preparation for nanometer hollow-structured materials. It is very important to control its decomposition rate, otherwise, it causes the collapse of hollow structure.

A number of researchers have investigated thermal decomposition and kinetics of $CaCO_3$ by employing a variety of techniques. Integral methods for determining the kinetic parameters[5–7] have been developed. Differential methods[8–12] have been adopted. The thermal decomposition of $CaCO_3$ under isothermal condition was studied [11]. It was found that the activation energy was 210.33 $kJ \cdot mol^{-1}$ for two-dimentional phase boundary movement and 201.65 $kJ \cdot mol^{-1}$ for the one-dimensional diffusion mechanism respectively. The intrinsic reaction rate constant was determined based on the grain model[12] and the activation energy (192 $kJ \cdot mol^{-1}$) was obtained. Gallagher and Johnson[13] demonstrated that the kinetics of decomposition of $CaCO_3$ was sensitive to the heat conductivity of the purge gas, and they concluded that the decomposition was controlled by heat transmission to the endothermic reactant. Criado and Ortega[14] observed that the apparent activation energy of $CaCO_3$ with particle size in the ranges 25—50 μm, 50—100 μm and 100—160 μm was lower than that of large particles. This behaviour may be explained by taking into account that the smaller the particle size, the greater the fraction of "$CaCO_3$ molecules" located on the surface with respect to the bulk. Therefore, the activation energy decreases because of the "extra" energy stored on the surface of the smaller particles. Chen *et al.*[15] have found that the initial decomposition temperature of cubic-shaped nano-sized $CaCO_3$ particles of mean size 20nm is substantially lower than that of bulk calcite when the heating rate is 10 $K \cdot min^{-1}$. Nano-sized particles (1—100 nm) that are in transitional region between molecular or atomic and macroscopic particles have peculiar physical and chemical properties such as ostensible, quantum and tunnel effects. However, very few have been reported on their thermal decomposition behavior.

In this paper, the mechanism of thermal decomposition and kinetic parameters of nano-sized $CaCO_3$

Received 2002-05-28, accepted 2003-01-14.

* Supported by the Key Research of Science & Technology of Education (No. 0202) and the Fundamental Research Plan of Huo Yingdong (No. 81063).

** To whom correspondence should be addressed.

will be discussed using Coats and Redfern's equation, master plots, kinetic compensation law and non-isothermal analysis.

2 THEORY

The reaction rate of a solid-state process can be described as

$$\frac{\mathrm{d}\alpha}{\mathrm{d}t} = kf(\alpha) \tag{1}$$

$$g(\alpha) = \int_0^\alpha \frac{\mathrm{d}\alpha}{f(\alpha)} \tag{2}$$

Arrhenius equation can be written as

$$k = k_0 \mathrm{e}^{-\frac{E}{RT}} \tag{3}$$

and Eq. (1) become

$$\frac{\mathrm{d}\alpha}{\mathrm{d}t} = k_0 \mathrm{e}^{-\frac{E}{RT}} f(\alpha) \tag{4}$$

If the temperature rises at a constant rate $\beta = \mathrm{d}t/\mathrm{d}t$, Eq. (4) can be integrated as

$$\int_0^\alpha \frac{\mathrm{d}\alpha}{f(\alpha)} = \frac{k_0}{\beta} \int_0^T \mathrm{e}^{-E/RT} \mathrm{d}T \tag{5}$$

In general, $E/RT \gg 1$, so that $\mathrm{e}^{-E/RT}$ can be expressed in Taylor series. By adopting the first derivative, we obtain

$$g(\alpha) = \frac{k_0 RT^2}{\beta E} \mathrm{e}^{-E/RT} \tag{6}$$

Eq. (6) can be rewritten as the Coats and Redfern's Equation.

$$\ln \frac{g(\alpha)}{T^2} = \ln \frac{k_0 R}{\beta E} - \frac{E}{R} \cdot \frac{1}{T} \tag{7}$$

If $g(\alpha)$ is known, the curves of thermogravimeteric analysis(TGA) can be used to calculate $\ln[g(\alpha)/T^2]$ for each possible controlling mechanism (as shown in Table 1). It was plotted against $1/T$ at different heating rate according to Eq. (7) and linear regression was used to determine the mechanism, and values of E and k_0.

3 EXPERIMENTAL METHODS

3.1 Synthesis of nano-sized $CaCO_3$ particles

Nano-sized $CaCO_3$ was prepared by reactive precipitation between $Ca(OH)_2$ and CO_2 in a rotating packed-bed (RPB) reactor. Calcium hydroxide was suspended in aqueous solution and was injected into the reactor with CO_2 simultaneously to perform the precipitation. $Ca(OH)_2$ was continuously recycled into the RPB reactor until neutral pH was reached. This indicates complete conversion of $Ca(OH)_2$ to $CaCO_3$. The calcium carbonate was filtered and then dried at 100℃. Detailed preparation method can be found in Chen *et al.*[18]. The nano-sized $CaCO_3$ was characterized by transmission electron microscopy for particle size analysis and X-ray diffraction for crystal structure determination.

3.2 Determination of decomposition kinetic parameters

Thermogravimetric analyzer (Model TASDT2960) was used to measure the sample mass as a function of time and temperature to a sensitivity of $\pm 10^{-5}$ g and ±0.001℃, respectively. In case of non-isothermal experiments, the sample was approximately 5 mg and the flow rate of nitrogen gas was 100 ml·min^{-1} at normal temperature and pressure. Experiments were conducted at heating rates of 5, 10 and 20 K·min^{-1}.

4 RESULTS AND DISCUSSION

The size of $CaCO_3$ particles produced with the RPB reactor was estimated to have a mean diameter of 20 nm and a narrow size distribution using transmission electron microscopy (TEM). The size and shape of the nano-sized precipitated $CaCO_3$ are illustrated in Fig. 1. The particles measured by X-ray diffraction is of calcite crystal structure as shown in Fig. 2.

The TGA profile of the non-isothermal decomposition of nano-sized $CaCO_3$ particles at different heating rate is shown in Fig. 3. $CaCO_3$ began to decompose into CaO and CO_2 at 640℃ when heating rate β is

Table 1 Kinetics of heterogeneous solid state reaction[16,17]

Mechanism		Symbol	$f(\alpha)$	$g(\alpha)$
diffusion				
one-dimensional transport process		D_1	$1/2\alpha^{-1}$	α^2
two-dimensional (cylinder without volume change).		D_2	$[-\ln(1-\alpha)]^{-1}$	$\alpha + (1-\alpha)\ln(1-\alpha)$
three-dimensional diffusion spherical symmetry (Jander mech.)		D_3	$1.5(1-\alpha)^{\frac{2}{3}}[1-(1-\alpha)^{\frac{1}{3}}]^{-1}$	$[1-(1-\alpha)^{\frac{1}{3}}]^2$
three-dimensional diffusion (Brounshtein-Ginstling mech.)		D_4	$2/3[1-\alpha)^{-\frac{1}{3}}-1]^{-1}$	$(1-2\alpha/3)-(1-\alpha)^{\frac{2}{3}}$
phase boundary movement	one-dimensional	R_1	1	α
	two-dimensional	R_2	$2(1-\alpha)^{1/2}$	$1-(1-\alpha)^{1/2}$
	three-dimensional	R_3	$3(1-\alpha)^{2/3}$	$1-(1-\alpha)^{1/3}$
nucleation and nuclei growth	$n=1$	A_1	$(1-\alpha)$	$-\ln(1-\alpha)$
(Avrami-Erofeev equ.)	$n=1.5$	$A_{1.5}$	$1.5(1-\alpha)[-\ln(1-\alpha)]^{\frac{1}{3}}$	$[-\ln(1-\alpha)]^{\frac{2}{3}}$

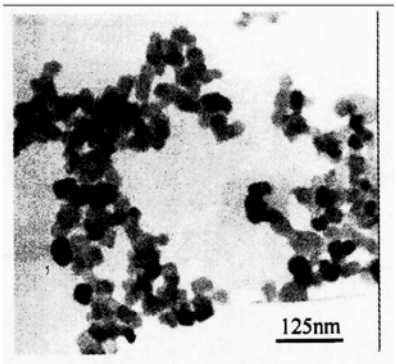

Figure 1 TEM photograph of $CaCO_3$ particles

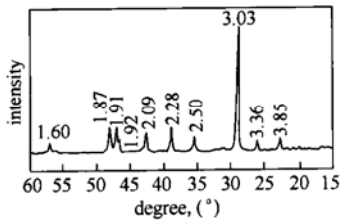

Figure 2 X-Pattern of $CaCO_3$ particles

5 K·min^{-1}, which is 180℃ lower than that reported for bulk calcite[19]. As heating rate increases, the decomposition temperature increases. It may be mainly reasoned that for non-isothermal process, solid decomposition temperature involves not only thermodynamics but also kinetics. The heating rate has an influence on the kinetic parameters, so that it leads to the different decomposition rate at different heating rate under the same temperature. Consequently it causes different TGA curves. The relationship between fraction decomposed and temperature is plotted in Fig. 4 for heating rates at 5, 10 and 20 K·min^{-1}. Since the sample is very little and granularity of nano-sized $CaCO_3$ is very tiny, the heat transport is neglected. It may be considered that the temperature of the sample is uniform. The values of $\ln[g(\alpha)/T^2]$ are plotted against $1/T$ at different heating rate for various mechanism models. The linear regression results of $\ln[g(\alpha)/T^2]$ against $1/T$ are shown in Table 2.

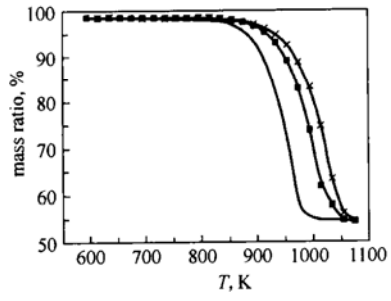

Figure 3 TGA curves at different heating rate
β, K·min^{-1}: —— 5; —■— 10; —×— 20

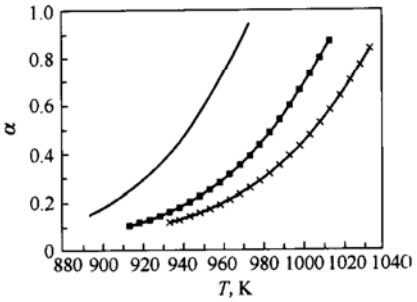

Figure 4 Relation of α *vs.* T
β, K·min^{-1}: —— 5; —■— 10; —×— 20

Table 2 Calculating results according to Eq. (7)

Mechanism	β, K·min^{-1}	E, kJ·mol^{-1}	k_0, s^{-1}	r
D_1	5	321.52	2.08×10^{18}	0.9998
	10	365.67	1.05×10^{20}	0.9994
	20	314.91	2.48×10^{17}	0.9998
D_2	5	357.46	1.37×10^{20}	0.9984
	10	365.67	1.05×10^{20}	0.9994
	20	335.09	1.76×10^{18}	0.9990
D_3	5	399.79	1.05×10^{22}	0.9933
	10	420.73	2.93×10^{22}	0.9955
	20	396.34	9.72×10^{20}	0.9940
D_4	5	370.93	2.04×10^{20}	0.9970
	10	383.82	2.46×10^{20}	0.9985
	20	366.42	2.10×10^{19}	0.9972
R_1	5	153.03	9.24×10^{8}	0.9998
	10	151.00	7.08×10^{8}	0.9996
	20	149.19	5.90×10^{8}	0.9998
R_2	5	181.56	2.54×10^{10}	0.9958
	10	188.69	4.26×10^{10}	0.9976
	20	179.90	1.48×10^{10}	0.9961
R_3	5	192.16	7.56×10^{10}	0.9928
	10	202.21	1.70×10^{10}	0.9952
	20	189.89	4.18×10^{10}	0.9961
A_1	5	215.08	5.38×10^{12}	0.9739
	10	231.71	3.52×10^{14}	0.9837
	20	136.87	1.79×10^{8}	0.9916
$A_{1.5}$	5	138.24	2.10×10^{8}	0.9835
	10	149.05	7.28×10^{8}	0.9873
	20	98.52	1.29×10^{7}	0.9857

In Table 2, it is in evidence that mechanism models of thermal decomposition of nano-sized $CaCO_3$ examed in this study can all be linearly fitted. Straight lines with high correlation coefficient (r) and low standard deviation were therefore selected to represent the possible mechanism. The correlation coefficients are all higher than 0.98 disregard the mechanism model chosen, which elucidate that the Coats and Redfern's equation is insensitive to the mechanism models studied.

Alternatively, many studies have employed reference theoretical curves namely "master plots"[20] to evaluate experimental data. Should the profile of a given set of experimental data be compatible with the master plot, the mechanism model is suitable. The master plot in this sense is a characteristic curve independent of experimental condition. The function

can be defined as follows

$$z(\alpha) = f(\alpha) \cdot g(\alpha) \tag{8}$$

If the heating rate is β and Eq. (4) can be integrated, Eq. (9) is obtained as below[19]

$$g(\alpha) = \frac{k_0 E}{\beta R} e^{-x} \left[\frac{\pi(x)}{x}\right] \tag{9}$$

where

$$\pi(x) = \frac{x^3 + 18x^2 + 88x + 96}{x^4 + 20x^3 + 120x^2 + 240x + 120} \tag{10}$$

and

$$x = E/RT \tag{11}$$

In this study, the fourth rational expression of Senum and Yang[21] is adopted to give errors lower than 10^{-7} for $x = 20$. Thus from Eq. (4), following equation can be obtained

$$f(\alpha) = \frac{e^x}{k_0} \frac{d\alpha}{dt} \tag{12}$$

Combining Eq. (9) and (12), we can be obtain

$$z(\alpha) = (d\alpha/dT)\pi(x)T \tag{13}$$

The master plots refer to the theoretical curves corresponding to Eq. (8), and the experimental data transformed using Eq. (13) are shown in Fig. 5. Comparing the master curves with the experimental curves for various mechanism models at different heating rates in Fig. 5, the reaction that follows either R_1 or D_1 mechanism is in good agreement with the non-isothermal experimental data.

The apparent activation energy of bulk calcite was reported to be 205 kJ·mol^{-1}[22] and 210 kJ·mol^{-1}[23]. The apparent activation energy (E) of nano-sized $CaCO_3$ in terms of mechanism D_1 was found in the range of 314.91—321.52 kJ·mol^{-1} as indicated in Table 2. These values are 1.5 times that of normal calcite, which is theoretically incorrect. This is because that the imbalance of atomic coordinate bond and the higher surface energy of nano-sized calcium carbonate will make the surface atoms too active to be stabilized, so that lower activation energy is required. Criado and Ortega[14]also noticed that small particles would cause the activation energy to decrease. The higher activation energy discovered with mechanism D_1 therefore nullifies the mechanism of one-dimensional diffusion parabolic law (D_1) for thermal decomposition of nano-sized calcium carbonate. On the other hand, the lower activation energy determined by mechanism R_1 in the range of 149.19—153.03 kJ·mol^{-1} supports the mechanism of one-dimensional phase boundary movement (R_1).

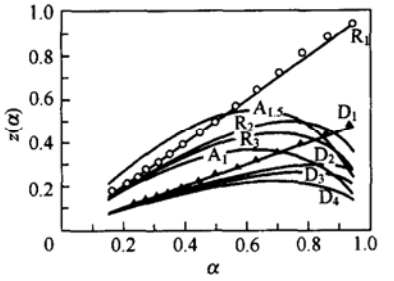

(a) $\beta = 5$ K·min^{-1}

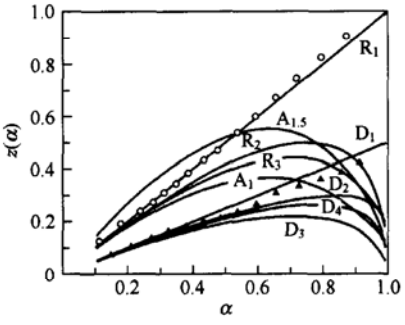

(b) $\beta = 10$ K·min^{-1}

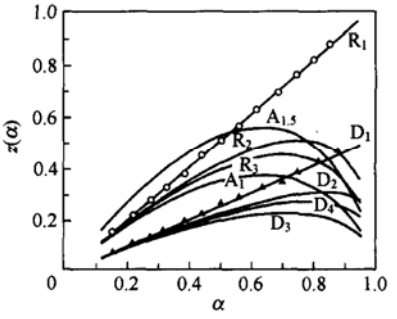

(c) $\beta = 20$ K·min^{-1}

Figure 5 Master curves $z(\alpha)$ *vs.* experimental curves at different heating rate
experimental values: ○ —R_1; ▲—D_1

According to the kinetic compensation law, the values of E and k_0 decrease with increase of β in the non-isothermal decomposition[24]. This is also observed with R_1 in Table 2. The mechanism R_1 is further shown to be consistent with the kinetic compensation law ($\lg k_0 = aE + b$), where a straight line is obtained as illustrated in Fig. 6.

The pre-exponential factors can serve as an accessorial criterion. According to the ionic vibration frequency[16], the value of pre-exponential factor of thermal decomposition may be in the vange of a few orders of magnitude around $10^9 s^{-1}$. The values of the pre-exponential factor k_0 is in the order of magnitude $10^9\ s^{-1}$ when the experimental data are evaluated by mechanism R_1.

From these experimental results we conclude that the thermal decomposition of the nano-sized calcium carbonate falls in the mechanism of one-dimensional (zero order) phase boundary movement (R_1) with E of

151 kJ·mol^{-1} and pre-exponential factor in the order of 10^9 s^{-1}.

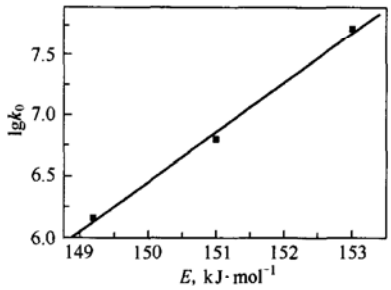

Figure 6 The plot of lgk_0 and E

5 CONCLUSIONS

The thermal behavior and mechanism of nano-sized $CaCO_3$ particles with mean diameter of 20 nm and narrow size distribution were studied using master plot, Coats and Redfern's equation and kinetic compensation law. The study shows that:

(1) Coats and Redfern's equation is an effective method to discriminate reaction mechanism of normal calcium carbonate or others solids, but it is difficult to determine a suitable mechanism for the thermal decomposition of nano-sized calcium carbonate.

(2) The nano-sized calcium carbonate decomposed at 640℃, which is 180℃ lower than that of normal calcite. The reason is that higher surface energy of nano-sized calcium carbonate makes the surface atoms too active to be stabilized.

(3) The thermal decomposition of nano-sized calcium carbonate is in line with the one-dimensional phase boundary movement (R_1). The apparent activation energy of nano-sized calcium carbonate is found to be 151 kJ·mol^{-1}, which is 50 kJ·mol^{-1} lower than that of calcite. The order of magnitude of pre-exponential factor is estimated to be 10^9 s^{-1}.

NOMENCLATURE

a, b	constants
E	apparent activation energy, J·mol^{-1}
$f(\alpha)$, $g(\alpha)$	functions depending on the process mechanism
k	rate constant
k_0	pre-exponential factor, min^{-1}
n	modeling parameter of Avrami-Erofeev equ.
R	gas constant, J·mol^{-1}·K^{-1}
T	absolute temperature, K
t	time, min
$z(\alpha)$	characteristic curve
α	fraction decomposed
β	heating rate, K·min^{-1}
r	correlation coefficient

REFERENCES

1 Zhu, X.D., Zhu, Z.B., Zhang, C.F., "Study of coal pyrolylic kinetics by thermogrametry", *J. Chem. Eng. Chinese. Univ.*, **13** (3), 223—228 (1999). (in Chinese)

2 Li, F., He, J., Du, Y.B., Evans, D.G., Wang, Z.X., Du, X., "Study on the preparation and non-isothermal kinetics of thermal decomposition of α-zirconium phosphate", *J. Inorg. Chem.*, **15** (1), 55—60 (1999). (in Chinese)

3 Li, L., Zhao, B.C., Yang, D., Li, X.R., "A method of characterizing the thermal decomposition and combustion stability of propellants", *J. Ballistics*, **11** (2), 27—31 (1999). (in Chinese)

4 Yu, J., He, J.S., "Non-isothermal crystallization behavior of maleic anhydride graft polypropylene and its ionomers", *Acta Poly. Sinica*, (5), 513—519 (1999). (in Chinese)

5 Horowitz, H.H., Metzger, G.A., "New analysis of thermogravimetric traces", *Anal. Chem.*, **35**, 1464—1468 (1963).

6 Coats, A.W., Redfern, J.P., "Kinetic parameters from thermogravimetric data", *Nature*, **201**, 68—69 (1964).

7 Zsako, J., "Kinetic analysis of thermogravimetric data", *J. Phys. Chem.*, **72**, 2406—2411 (1968).

8 Newkrik, A.E., "Thermal methods of analysis", *Anal. Chem.*, **32**, 1558—1563 (1960).

9 Ingraham, T.R., Marier, P., "Activation energy calculation from a linearly-increasing temperature experiment", *Can. J. Chem. Eng.*, **42**, 161—163 (1964).

10 Sharp, J.H., Wentworth, S.A., "Kinetic analysis of thermogravimetric data", *Anal.Chem.*, **41**, 2060—2062 (1969).

11 Mulokozi, A.M., Lugwisha, E., "New aspects of the decomposition kinetic of calcite I. Isothermal decomposition", *Thermochimica Acta*, **194**, 375—383 (1992).

12 Rao, T.R., "Kinetic parameters for decomposition of calcium carbonate", *Can. J. Chem. Eng.*, **71** (3), 481—484 (1993).

13 Gallagher, P.K., Johnson, D.W., "The effects of sample size and heating rate on the kinetic of the thermal decomposion of $CaCO_3$", *Thermochimica Acta*, **6**, 67—83 (1973).

14 Criado, J.M., Ortega, A., "A study the influence of particle size on the thermal decomposion of $CaCO_3$ by means of constant rate thermal analysis", *Thermochimica Acta*, **195**, 163—167 (1992).

15 Chen, J.F., Jia, Z.Q., Wang, Y.H., Zheng, C., "Synthesis and characterization of cube-shape $CaCO_3$ nanometer paticles in high gravity field", *Chinese J. Chem. Phy.*, **10** (5), 457—460 (1997). (in Chinese)

16 Zou, W.Q., Feng, Y.J., "Study on non-isothermal kinetics of thermal decomposition of $NaHCO_3$", *J. East China Institute of Chem. Tech.*, **14** (2), 158—163 (1988). (in Chinese)

17 Ahmed M., Gadalla, "Kinetics of dissociation of hydrated cerium (Ⅲ) sulfate, nitrate and oxlate in air", *Thermochimica Acta*, **95**, 179—200 (1985).

18 Chen J.F., Wang, Y.H., Guo, F., Wang, X.M., Zheng, C., "Synthesis of nanoparticles with novel technology: High-gravity reactive precipitation", *Ind. Eng. Chem. Res.*, **39**, 948—954 (2000).

19 Dean, J.A., Lange's Handbook of Chemistry, 15th ed., McGraw-Hill Book Co., Section 3, 21 (1999).

20 Criado, J.M., Malek, J., Ortega, A., "Applicability of the mater plots in kinetic analysis of non-isothermal date", *Thermochimica Acta.*, **147**, 377—387 (1989).

21 Senum, G.I., Yang, R.T., "Rational approximations of the integral of the arrhenius Function", *J. Therm. Anal.*, **11** (3), 445—447 (1977).

22 Beruto, D. Searcy, A.W., "Use of Langmuir method for kinetics studies of decomposition reacion: Calcite ($CaCO_3$)", *J. Chem. Soc. Faraday Trans.*, **17** (12), 2145—2153 (1974).

23 Reading, M., Dollimore, D., Rouquerol, J., Rouquerol, F., "The measurement of meaning fulactivation energies using thermoanalytical methods: A tentative Proposal", *J. Therm. Anal.*, **29** (4), 775—785 (1984).

24 Li, J.H., Zhang, N., Cheng, Q.T., "Identification of mechanism and investigation on the kinetics of thermal dehydration of barium oxalate hemihydrate", *Acta Chimica Sinica*, **51**, 550—555 (1993). (in Chinese)